Wesleyan University | The Honors College

Hot Planets, Hot Stars: Searching for Transiting Exoplanets Using TESS and Wesleyan's Automated Telescope

by

Uday Shankar Narayanan
Class of 2024

A thesis submitted to the
faculty of Wesleyan University
in partial fulfillment of the requirements for the
Degree of Bachelor of Arts
with Departmental Honors in Astronomy

Middletown, Connecticut | April, 2024

Abstract

Bright, hot stars present challenges in finding their exoplanets using the radial velocity and transit techniques. Finding exoplanets around these stars would enable high precision atmospheric characterization with less interference of stellar activity. They may also represent a different class of planetary atmospheres, driven by a very different stellar spectrum than cool star hosts. We aim to search for planets in this parameter space by monitoring bright ($V < 7$), hot (Teff > 6500 K) stars and cross referencing those targets with observations collected by TESS (Transiting Exoplanet Survey Satellite). We obtain long duration observations with Wesleyan's automated 24-inch telescope and couple that with TESS light curves of the same objects. In particular, we observe long-period and single-transit candidates with host stars in this parameter space. We present observed light curves and candidate systems. Additionally, we characterize the observed stellar variability and evaluate the probability of detecting an additional transit. While it is difficult to detect planets orbiting bright, hot stars, it should be possible to find warm Jupiter-sized planets. This population provides clues to the formation and evolution of planetary systems orbital elements and, when transiting a bright star, are excellent targets for atmospheric characterization.

"I've got the sauce."

–Kiryu Kazuma,

"*Ryū ga Gotoku 3*"

Acknowledgments

Firstly, I'd like to thank Cassidy Soloff. If I hadn't seen you present your thesis work at an astronomy club meeting, I not sure I would have pursued exoplanet research. From the bottom of my heart, thank you so much for your inspiration.

Thank you Seth Redfield for being an incredible advisor and mentor to me. From Astronomy 155 to now, you've helped me grow from a curious student to an astronomy researcher. I truly could not have made it here without your guidance.

Thank you Kyle McGregor for showing me the ropes when I first started to use the 24-Inch telescope. You really helped get me into the research process as seamlessly as possible, and I really appreciate the help you gave me.

Chris Tian. What do I even say? For starters, my research would be basically nonexistent without your help operating the telescope, so I can't thank you enough for that. Beyond that, though, you've just been an incredible friend and guiding light. You've helped me make certain decisions in life that I don't know I could have made otherwise. There are simply no words I can say that can properly express the impact you've had on me. I guess you really are kind of the best.

To my family, thank you for always believing in me. I love you all to the stars and back.

Contents

Chapter 1

Introduction

1.1 Exoplanets

For a good part of humanity's existence, the only planets known to exist were the eight located within our solar system. We surmised for centuries that other worlds could exist beyond what appeared to the naked eye, but for the longest time, we lacked conclusive evidence. Three decades ago, that changed when researchers observed an odd pattern coming from the pulsar PSR 1257+12 in the Milky Way (Wolszczan & Frail 1992). The rotation of the star's emanating jets were varying in period, far beyond what any observational error could account for. Intrigued by this oddity, researchers made a stunning conclusion: this peculiar pattern was caused by none other than the gravitational influence of two planets orbiting the star, each multiple times the mass of Earth (Wolszczan & Frail 1992). This discovery proved to be monumental, setting the foundation for the field of exoplanet science and ushering in an era of rapid exoplanet discovery that spanned the decades to follow. Since then, the field has greatly matured and our understanding of exoplanet properties with it, owed to clever methods applied by researchers like the radial velocity and transit methods, as well as the advent of new advanced telescopes like *TESS* (Transiting Exoplanet Survey Satellite) and *JWST* (James Webb Space Telescope).

1.2 Hot Jupiters

Due to their large radii and masses, some of the earliest planets to be detected were hot Jupiters (Mayor & Queloz 1995): massive gas giants with high temperatures ($\geq$ 1600K; Fortney et al. (2021)) orbiting close to their host stars ($\leq$ 0.1 AU; Maldonado, J. et al. (2018)). The discovery of these planets was initially a surprise as our models for planetary formation did not support their existence. This was due to our presumption that the gasses that make up gas giants can only coalesce in regions further out from their host stars, where gasses condense into ices and large quantities can be accreted. The contradiction between theory and observation incited an investigation into the existence of hot Jupiters, and since then, large strides have been made in explaining their existence. As of today, there are three main hypotheses.

One hypothesis is that the planets simply formed close to the star, accreting matter from the inner zones of the star's proto-planetary disk. This is the least likely of the hypotheses given that these zones are not ideal for the high volume mass accretion necessary for gas giant formation (Johansen & Lambrechts 2017). More likely is the possibility that these planets have migrated. This idea of migration is the crux of two other hypotheses; one posits that the gas giants formed further out in the solar system, then migrated inward due to torques from the proto-planetary disk (Baruteau et al. 2014). Another suggests that these planets started out with highly eccentric orbits that ended up stabilizing near the star due to tidal dissipation (Jackson et al. 2021). At present, research is being done to verify the accuracy of these hypotheses, and the strength of that research is dependent on data from large populations of hot Jupiters. The more of these planets we can find and categorize, the closer we get to understanding their origin.

1.3 Exoplanet Detection Methods

When it comes to detecting exoplanets, there are two main methods: the radial velocity method and the transit method.

The radial velocity method uses our understanding of orbital dynamics coupled with the Doppler Effect to determine a planet's existence. Saying that a planet orbits a star is largely true, but if we are to be precise, both the star and the planet orbit the center of mass between them. The reason we do not often make this distinction is because this center of mass is usually not far off from the center of the star. However, in the case of large planets, the center of mass, also known as a barycenter, can be far enough from the star's center that its orbital motion is detectable. How this detection works is that the spectrum of a star is taken over time, and if there is a change in that spectrum with respect to wavelength, there potentially exists a planet. This is where our understanding of the Doppler Effect comes into play. When a star orbiting a barycenter moves in our direction, we see its light at a shorter wavelength than if it were still; the inverse also applies. This means that when taking spectra, we can see these wavelength changes as shifts in the spectra, and from those shifts, we can discern variations in radial valocity and detect a planet, as can be seen in Figure 1.1. Additionally, we can discern some of the planet's properties, specifically its period, lower mass limit, and eccentricity.

The transit method is rather simple in principle; it takes advantage of the idea that when a light source is partially blocked, it emits less light. By that same logic, a star's observed brightness decreases when it is partially eclipsed by a planet passing in front of it. Using a telescope, this decrease in light intensity can be measured as a dip in a star's photon flux as shown in Figure 1.2.

If multiple of these flux dips are detected when observing a star, there is

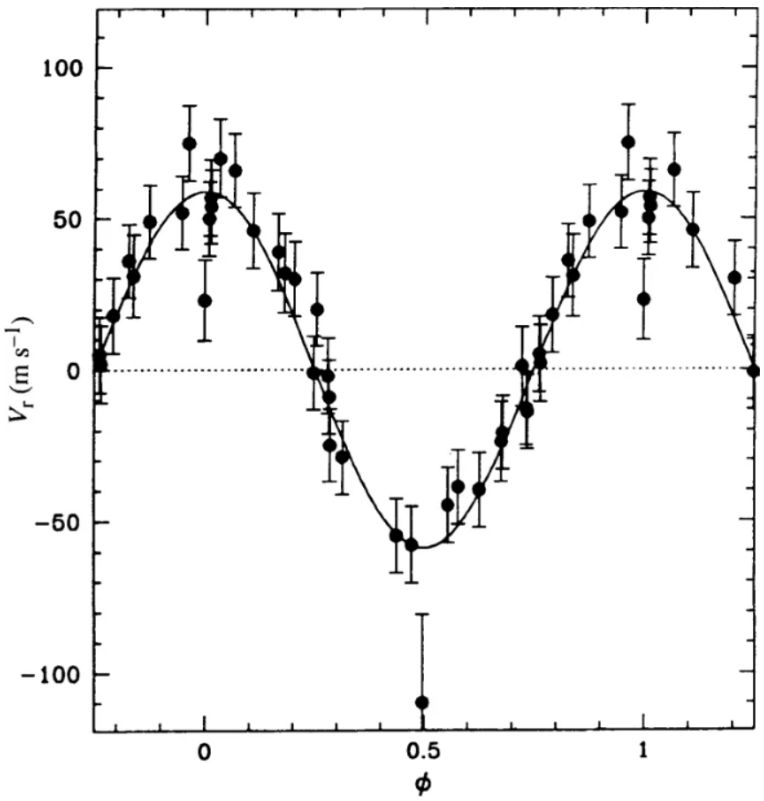

Figure 1.1: Sinusoidal variation in the radial velocity of 51 Peg, indicating the presence of a planet (Mayor & Queloz 1995).

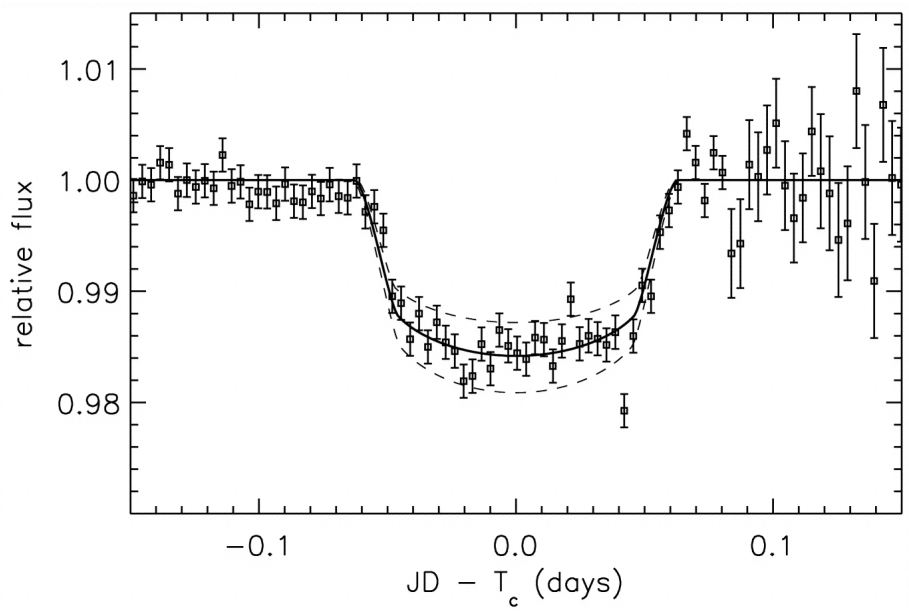

Figure 1.2: Light curve of a planetary transit (Charbonneau et al. 2000).

enough data to confirm the discovery of a planet and measure its period and radius, relative to its host star. The simplicity of this process, coupled with the design and launch of multiple transit missions along with several ground-based surveys, is why, to date, the transit method is the most successful and widely-used technique for detecting exoplanets. Despite this effectiveness, however, the method still has its limitations.

One of these limitations is that it's only useful for edge-on planetary systems, meaning that planets' orbital planes have to align with our line of sight for us to see them. Another limitation is that the window for transit detection is often very small. For example, if we were to observe the transits of planets within our solar system from an outside perspective, Figure 1.3 shows how miniscule their transit durations would be relative to their periods.

Planet	Transit Depth $\Delta L/L$ (%)	Transit Duration t_C (hours)	Orbital Period (years)	Orbital Radius R (AU)	Geometric Probability d*/D (%)	Inclination to Ecliptic (degrees)
Mercury	0.0012	8.1	0.241	0.39	1.19	7.0
Venus	0.0080	11.0	0.615	0.72	0.65	3.4
Earth	0.0084	13.0	1.00	1.00	0.47	0.0
Mars	0.0023	16.0	1.88	1.52	0.31	1.9
Jupiter	1.01	30.	11.86	5.2	0.089	1.3
Saturn	0.68	40.	29.5	9.5	0.049	2.5
Uranus	0.116	57.	84.0	19.2	0.024	0.8
Neptune	0.096	71.	164.8	30.1	0.015	1.8

Figure 1.3: Transit Properties of planets in our solar system (Borucki et al. 1996).

Using the radial velocity method, you collect data over large stretches of time, and only after collecting all that data are you able to finally determine whether a planet exists; because of these long observational periods, data collection is fairly spaced out, leaving room for gaps between observations. With the transit method, you need to observe the moment that transit starts (called ingress), the full transit, and the moment transit ends (called egress); each of these processes

can take only a few hours, which can make the window for detection really small. The only way to account for this is to continually collect stellar data at every possible moment, and even then, ground based observatories are limited by the hours of night.

This is ultimately what makes space-based observatories like *TESS* so powerful. They do not have to worry about the time of day, so they can leverage all of the strengths of the transit method, while getting around one of its biggest restrictions. Additionally, these satellites are able to monitor the flux of multiple stars at once (about 15,000 per sector for TESS; Swade et al. (2019)), possibly discovering multiple exoplanets in the process.

1.4 F-stars

There is one caveat to these multi-star observations, though, which is that hot, bright stars are oftentimes less observed by these surveys, which can be seen in Figure 1.4.

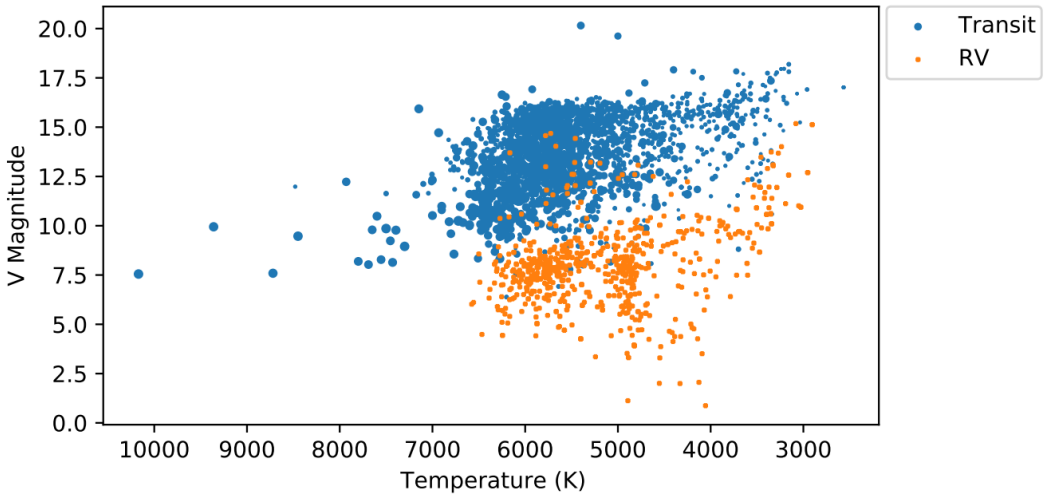

Figure 1.4: Detected exoplanets plotted by V magnitude and Temperature (Soloff & Redfield 2022).

This is due to the goal of these surveys being to observe as many stars as possible. In general, most of the stars in the night sky are distant and by extension, dimmer. Additionally, hot, bright stars, like F-stars, are in the minority, compared to the fainter M and K-stars. Because of this, telescope exposure times are evaluated based on distant, medium-brightness stars, which means that high-brightness stars end up being overexposed like can be seen in Figure 1.5.

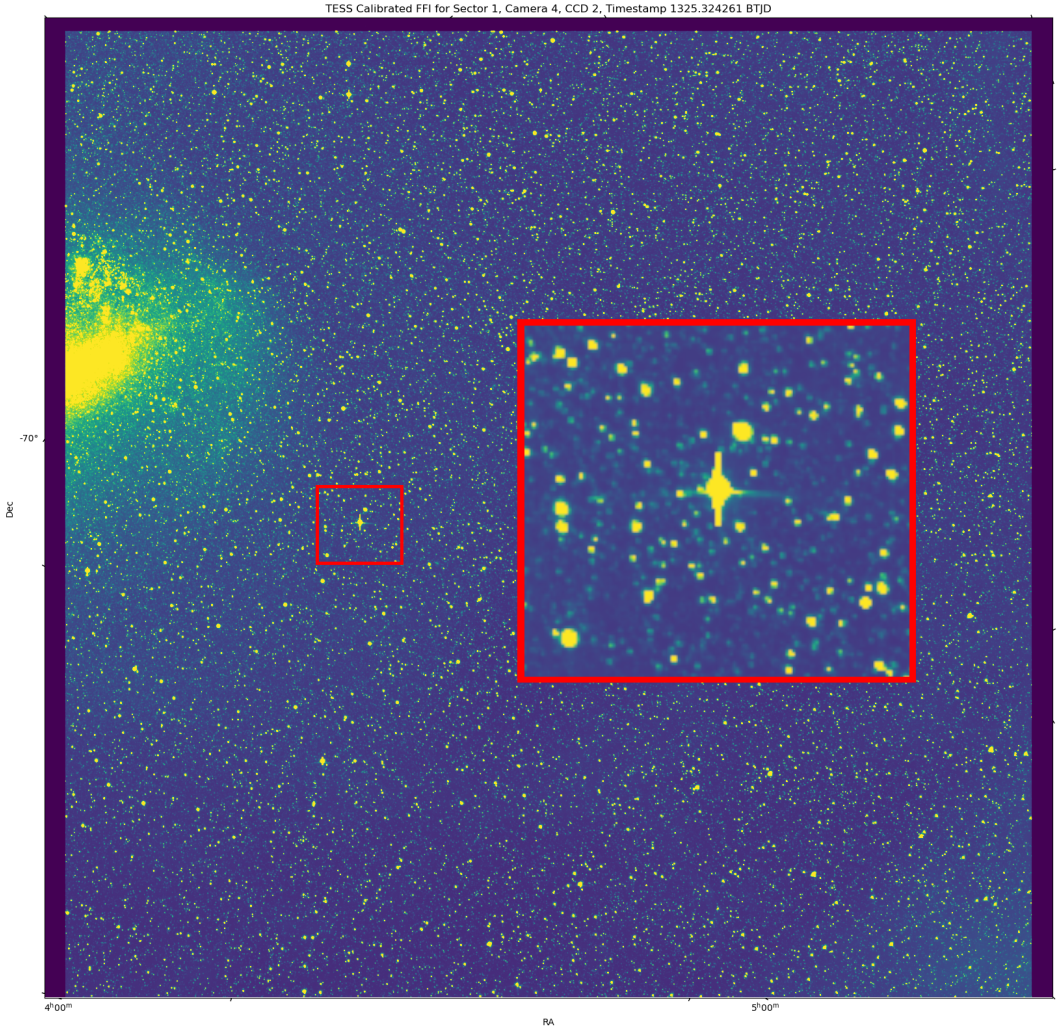

Figure 1.5: A full frame image from *TESS*, showing an overexposed star.

This is not to say that these kinds of stars are not observed by surveys, just that they are observed far less often. In this respect, ground-based observatories have

an advantage: they are not beholden to observing as much of the sky as possible, meaning that they can be used to manually perform follow-up observations on bright stars to make up for time lost on surveys. This is the philosophy that guided the work of my predecessor, Cassidy Soloff, in his 2022 research which centered around the search for hot Jupiters around hot, bright stars (Soloff & Redfield 2022).

1.5 Previous Work

Soloff & Redfield (2022) put together a list of observable F stars, along with their properties. Some of these properties included brightness (Vmag < 8), temperature (Teff > 6500K), number of hours in the sky, number of reference stars, and orbital inclination. In their pilot study, they hand selected a few targets, specifically stars that were hot and bright enough to have not been observable in previous transit or RV surveys, but also observable from Wesleyan's Van Vleck Observatory. These stars were HD 32715, HD 206751, HD 6314, and HD 21844. For time periods ranging from a few days to a few months, they observed these targets using Wesleyan's 24-inch telescope. Initial observations showed little variations in flux from HD 32715 and HD 206751. HD 6314 had quite a lot of flux variance, but that variance was too large, indicating that the star itself was the source of the fluctuations. The only target that showed promise in hosting an exoplanet was HD 21844 when on the night of January 25th, 2022, they observed a dip in stellar flux seemingly matching that of an exoplanet transit curve. Unfortunately, the data was not collected for long enough to see the full potential transit, just a partial one. Regardless, this data made future observations of HD 21844 a priority, which led to its monitoring from that point on. Seven months

after the observation of HD 21844's potential transit, I joined the project, intent on further investigating the star as well as expanding our search beyond it.

1.6 Overview

While *TESS* observes F-stars less frequently than other kinds of stars, it still can prove incredibly useful as a guide for future observations. For in-progress transit searches, *TESS* data can be used to follow up on targets. Additionally, *TESS* can be used to start these searches as well. There are many stars that *TESS* has observed single transits for (Yao et al. 2021), and some of these stars are hot Jupiters that can be observed from Van Vleck Observatory. Consequently, *TESS*, when paired with the observational ability of Wesleyan's 24-inch telescope, has the potential to greatly expedite the discovery of Jupiter-sized planets around hot, bright stars.

Chapter 2

Instruments

On a data-recording level, both Wesleyan's telescope and *TESS* are rather similar. Despite their differences in size, specifications and operating locations, they are both image the sky and record their observations using CCDs, or charge coupled devices. This design similarity is owed to CCDs' effectiveness in converting photon input from observations into digital images. To get more specific, when a telescope observes a patch of sky, the light from that observation is projected onto the CCD's sensor grid. These sensors then convert the amount of photons they receive into a corresponding amount of electrical charge; this enables the creation of a digital image based on light levels.

	24-Inch Telescope	*TESS*
Field of View	0.4°x 0.4°	24°x 96°
Focal Ratio	f /6.5	f /1.4
Pixel Resolution	2048 x 2048	4096 x 4096

Table 2.1: Specifications of each telescope.[1] [2] Ricker et al. (2014)

2.1 24-Inch Telescope

Wesleyan's main telescope for observational research, as shown in Figure 2.1, is a 24-inch PlaneWave Instruments reflecting telescope. This telescope is robotically

[1] https://planewave.com/product/cdk24-ota/
[2] https://www.flicamera.com/spec_sheets/archive/PL4240.pdf

controlled from a computer, which sets up observations using a scheduling system. Observations are recorded by a 2048 x 2048 CCD, which then digitally outputs these observations as FITS (Flexible Image Transport System) files.

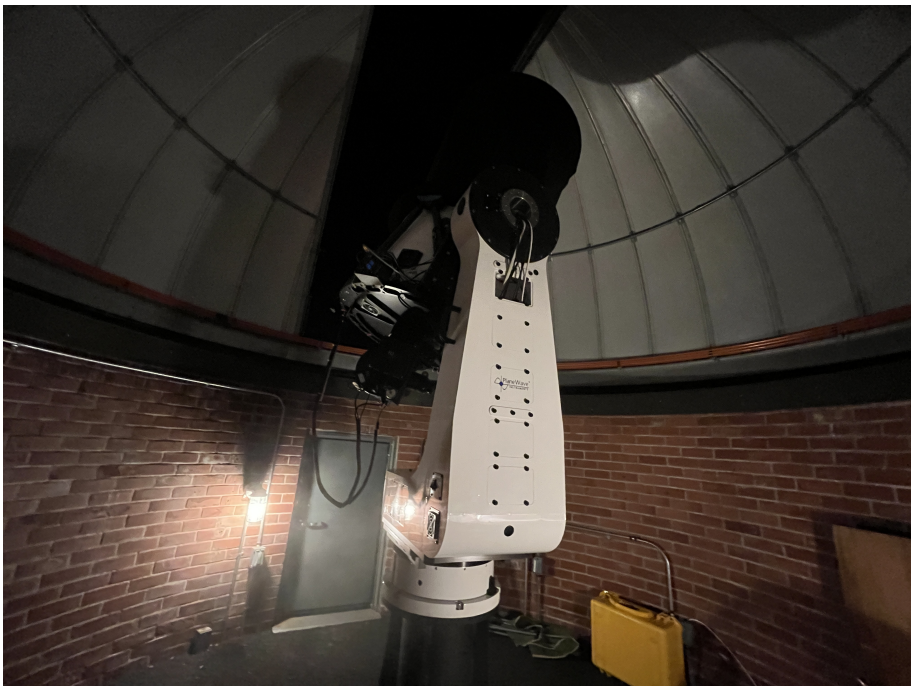

Figure 2.1: Wesleyan's 24-Inch Telescope.

2.1.1 Advantages of the 24-Inch Telescope

The biggest advantage of using this system is having complete control over observation parameters. Because each observation has to be set up manually, settings like exposure time and number of exposures can be finely tuned for each star. Additionally, once these parameters are set, they can be put into an ACP scheduler, which will then prompt the telescope to observe a target automatically when conditions are favorable. What defines these favorable conditions can also be adjusted. For instance, if there is a specific range of dates that a star needs to be observed for, these dates can be input into the scheduler. Acceptable weather

conditions for observations can also be adjusted, albeit more manually. This is possible due to the telescope computer's connection to a weather station on the roof of Wesleyan's observatory. Because this weather system errs on the side of caution to protect the telescope, it can sometimes close the telescope on nights when it does not need to, which is why controlling the acceptable/unacceptable weather threshold can be useful.

2.1.2 Disadvantages of the 24-Inch Telescope

The downsides of this system are shared with all ground based telescopes in general. While a certain level of atmospheric noise can be accounted for during observations, the telescope can't account for more drastic conditions like clouds, intense fog, or precipitation. This greatly limits observable nights and can make planning observations a complicated process. Another downside is the system's inability to observe targets for sustained periods, like days or weeks. This is unsurprisingly due to sunlight getting in the way of observations during the day. These limitations are quite drastic and greatly slow research progress, but where this telescope fails, *TESS* is able to pick up some of the slack.

2.2 *TESS*

Shown in Figure 2.2, *TESS* or the *Transiting Exoplanet Survey Satellite* is a space telescope that was launched in 2018 (Ricker et al. 2014). Its goal is to survey thousands of stars for long periods of time and discover exoplanets around them using the transit method. For data collection, *TESS* observes multiple stars in sectors of the sky for a given time, then outputs that data in the form of photometric light curves.

2.2.1 Advantages of *TESS*

Having been constructed for wide-field photometry, *TESS* immediately has an advantage with its field of view, carrying four lenses for a combined field of view of 24°× 96°, as can be seen in Table 2.1. Its data is also prone to less disturbances, which is owed to its presence in Earth orbit; light from stars is more effectively seen without atmospheric noise or weather events obscuring it. This also means that time of day isn't an issue, meaning that *TESS* can get target data for weeks on end and make planetary searches much more efficient.

2.2.2 Disadvantages of *TESS*

Because *TESS* is a survey satellite, meant to observe multiple targets at once, it invariably observes more medium-brightness stars, compared to brighter ones. This leads to overall shorter observational periods for bright stars, which makes finding transits rarer. The time in between observations of a given sector of sky can also be long, potentially months or even years apart, further exacerbating the lack of data for bright stars. In this aspect, the 24-inch is useful, getting data over long periods of time, even if it only intermittently.

2.3 The Power of Two

Both of these telescopes are powerful research instruments in their own right, but they each have their sets of weaknesses. These weaknesses, however, can be partially circumvented by using both tools in conjunction with one another. *TESS* can observe bright stars for long time periods continuously, while the 24-

[3]https://svs.gsfc.nasa.gov/vis/a010000/a012700/a012782/TESS_alone_high_res.jpg

inch telescope can collect further data after *TESS*'s data collection period has ended.

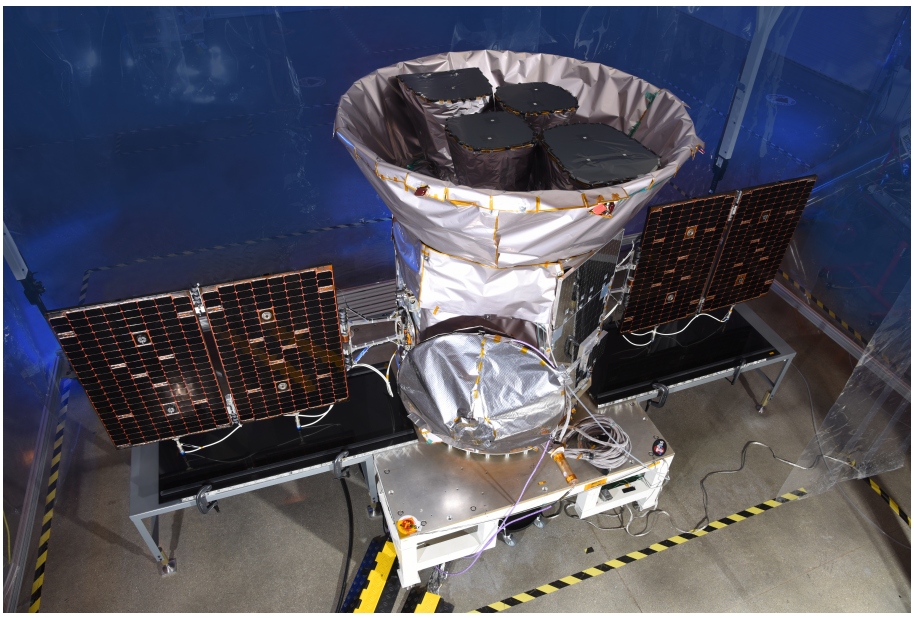

Figure 2.2: *Transiting Exoplanet Survey Satellite.* [3]

Chapter 3

Data

3.1 24-Inch Telescope

3.1.1 FITS

FITS (Flexible Image Transport System) is the file format that observations using Wesleyan's telescope are recorded in. Encoded in each FITS file is an array, containing light level readouts from a telescope's CCD; this standard format can be read by multiple softwares as an image. The resolution of this image is dependent on the arrangement of the sensors on the CCD that captures it. For instance, a CCD with a 1024 sensor width and 1024 sensor length produces a 1024 x 1024 pixel image. (Wells et al. 1981)

Additionally, the files' headers, as seen in Figure 3.1, include a multitude of useful information, including the image exposure time, date observed, and object observed. This information can be easily accessed using code, which makes sorting through a large amount of FITS files and getting their information a relatively simple process.

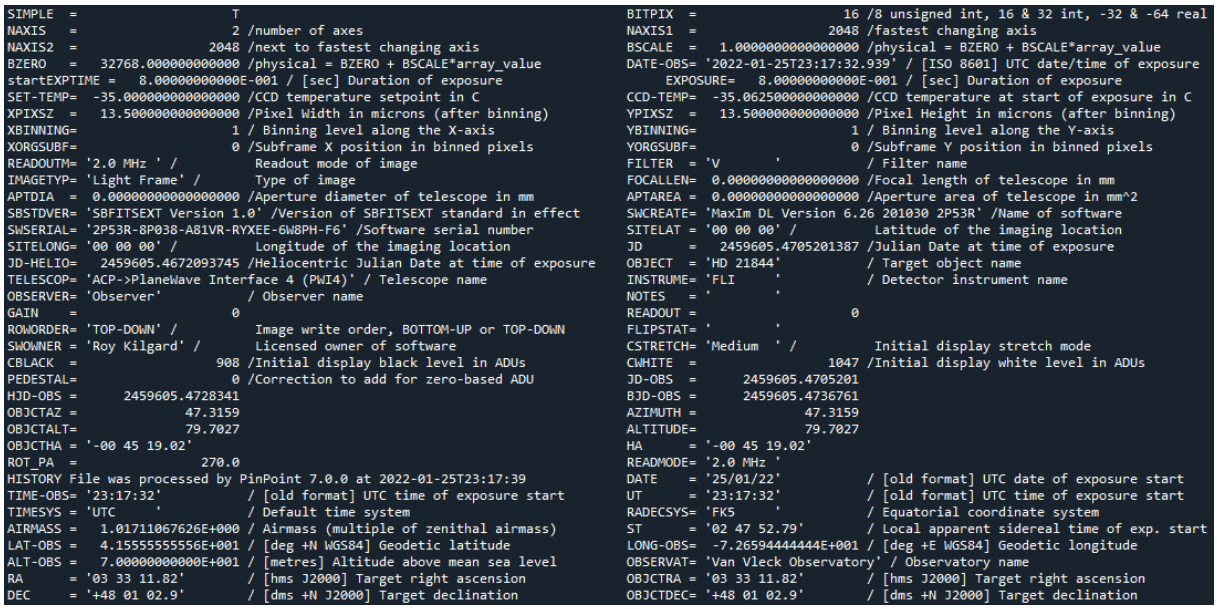

Figure 3.1: Information encoded in FITS header.

3.1.2 AstroImageJ

AstroImageJ is a software package capable of reading FITS files and performing various data reduction techniques on them. (Rodriguez et al. 2016) It has been applied heavily in this research project, owed in no small part to its ability to perform multi-aperture photometry.

Before getting into what multi-aperture photometry is, however, it is important to establish how AstroImageJ import FITS files. For a given interval in which a telescope observes an object, multiple FITS files like seen in Figure 3.2 are generated depending on how many exposure times fit into that interval. AstroImageJ allows these files to be imported in the style of a movie, allowing for playback of the entire observation; this is incredibly useful as it allows for an efficient cleanup process. By cleanup, I refer to the removal of unusable FITS files caused by anything from telescope movement to weather or sometimes even cosmic rays hitting the CCD. After this cleanup process finally comes the process of multi-aperture

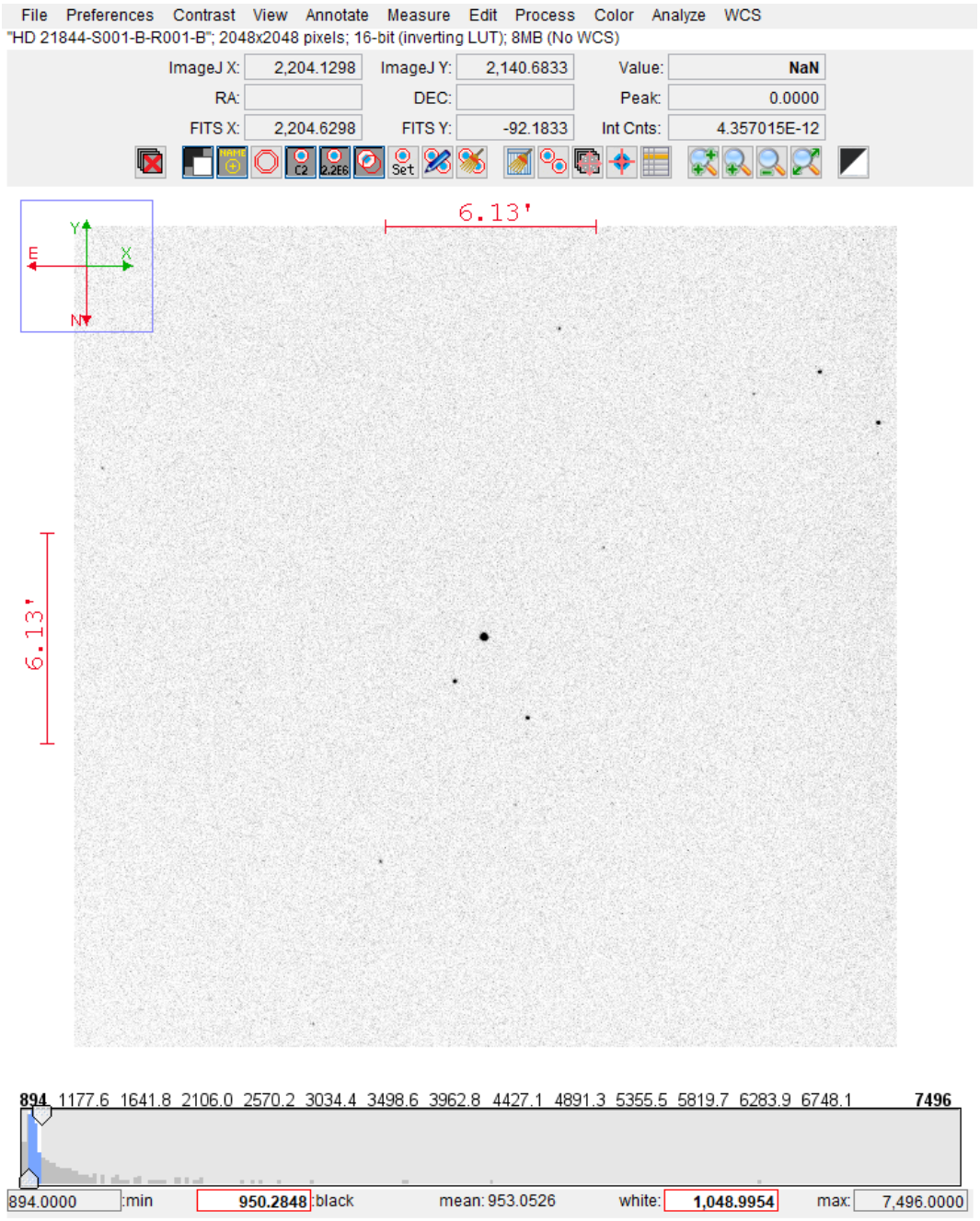

Figure 3.2: FITS file of a 0.8 second exposure of HD 21844 accessed in AstroImageJ. The image has a pixel resolution of 2048 x 2048. The field of view is 45 x 45 arcminutes.

photometry.

Multi-aperture photometry is the process of measuring the light flux of a single star over time, relative to other stars captured in the same observation. This kind of data reduction is ideal for this research project because the absolute light flux of a star is not relevant when using the transit method; all that matters is that the flux changes in a way that indicates stellar occlusion from a planet.

But why use other stars as reference instead of only measuring the target star's flux? The answer is that using other stars as reference is more reliable with ground-based observations that observe through the atmosphere. When observing stars from Earth, the atmosphere often interferes with data collection, whether in the form of small fluctuations or more drastic weather conditions. Measuring a target star along with its surrounding stars allows for the normalization of the target star's light curve over time. This is because the circumstances affecting its observed flux also affect the other stars' fluxes. Figure 3.3 shows how the large-scale deviations for 4 stars' lightcurves look similar for a given observation.

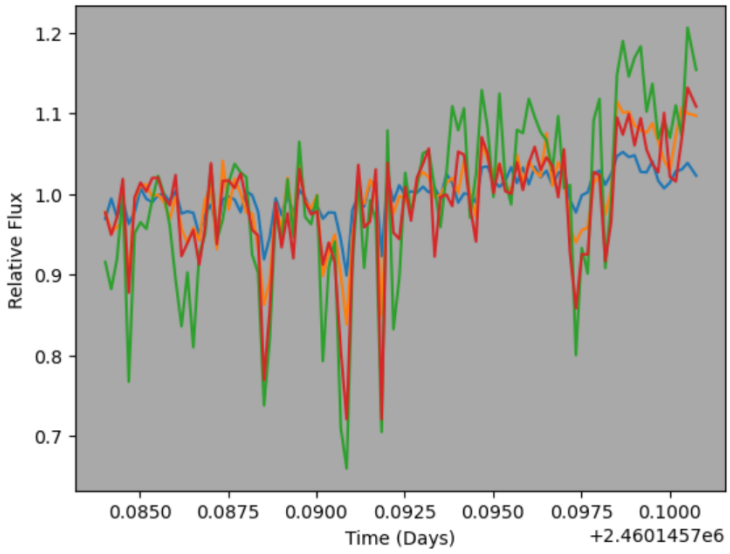

Figure 3.3: Flux changes for 4 stars over a single observation.

Now that we understand the basics of multi-aperture photometry, we can get into how it is done in AstroImageJ. To start, centroid apertures are placed onto stars in the FITS images. What these apertures do is mark a circular radius in which the light levels from all of the enclosed pixels are measured. The first of these apertures is placed on the target star, while the other apertures are placed on surrounding stars in the same observation, as shown in Figure 3.4.

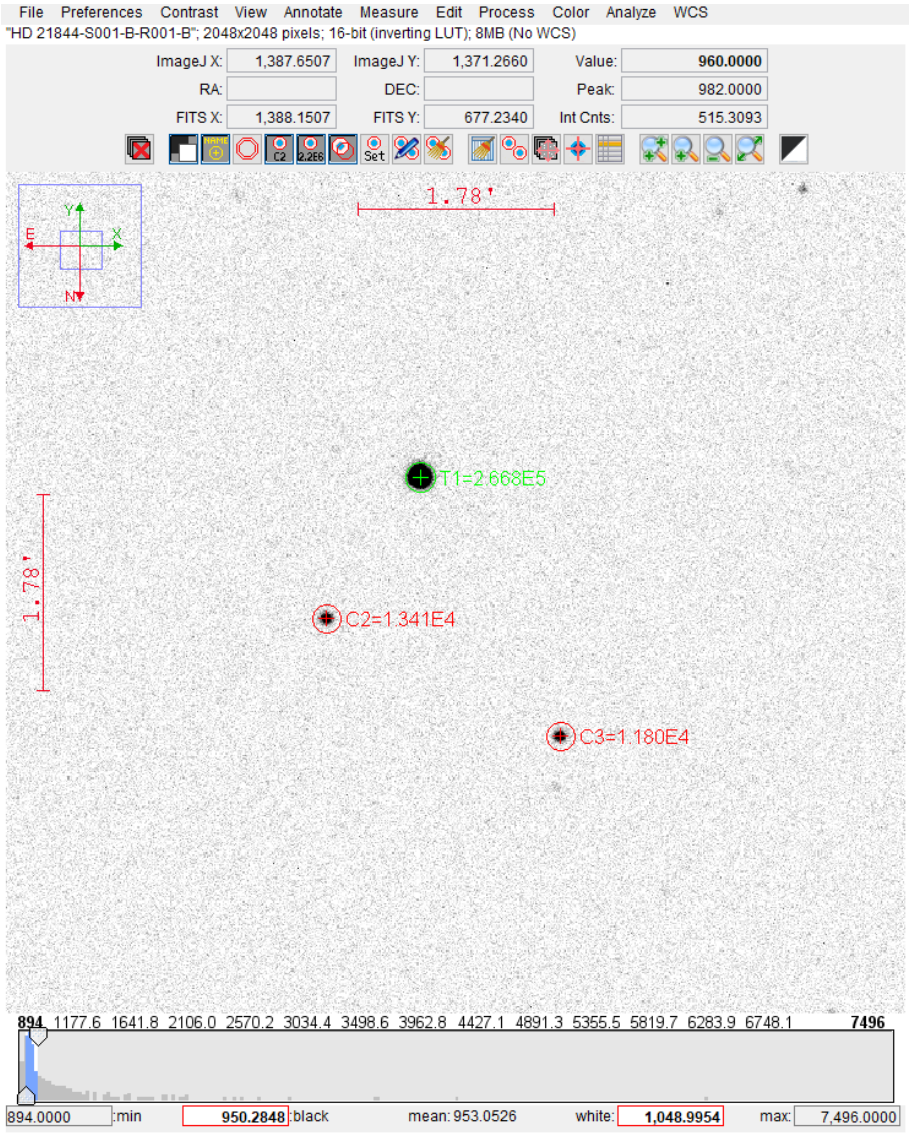

Figure 3.4: Zoomed-in version of Figure 3.2 with apertures placed on 3 stars. These apertures have a 9-pixel radius.

After that, the program automatically performs multi-aperture photometry for every FITS image in a sequence, outputting that data into a table. The data can then be further analyzed using a programming language like Python.

3.2 *TESS*

3.2.1 MAST

MAST is an online archive, hosting observation data from high profile space missions like *JWST*, *Hubble*, *Kepler*, and *TESS*. This data comes in many forms, depending on the telescope. In the case of *TESS*, there are four different data product types: target pixel files, data validation time series, calibrated full frame images, and extracted light curves. While we could repeat the same data reduction process by doing photometry on full frame images, it is much easier to use the pre-reduced light curves. These light curves can be accessed using the astropy package in Python, which allows us to find them using the name of our target star.

3.2.2 Light Curves

The light curve data products themselves are plots with time in days on the x-axis and flux in electrons s^{-1} on the y-axis, as seen in Figure 3.5. The amount of days that a target is observed varies depending on its position in the sky, but given that the shortest campaigns last 27 days, there is a wealth of data to examine regardless. (Ricker et al. 2014) Additionally, because *TESS* is in space, it is able to measure the absolute flux of a star with minimal noise. The only caveats to this are points at which *TESS* stops or begins recording data, in which case, the flux

either spikes or dips dramatically. This is likely a result of mechanical interference from the telescope itself.

Additionally, some of these light curves are reduced using eleanor, a tool that extracts data products and applies systematic corrections to the data. (Feinstein et al. 2019)

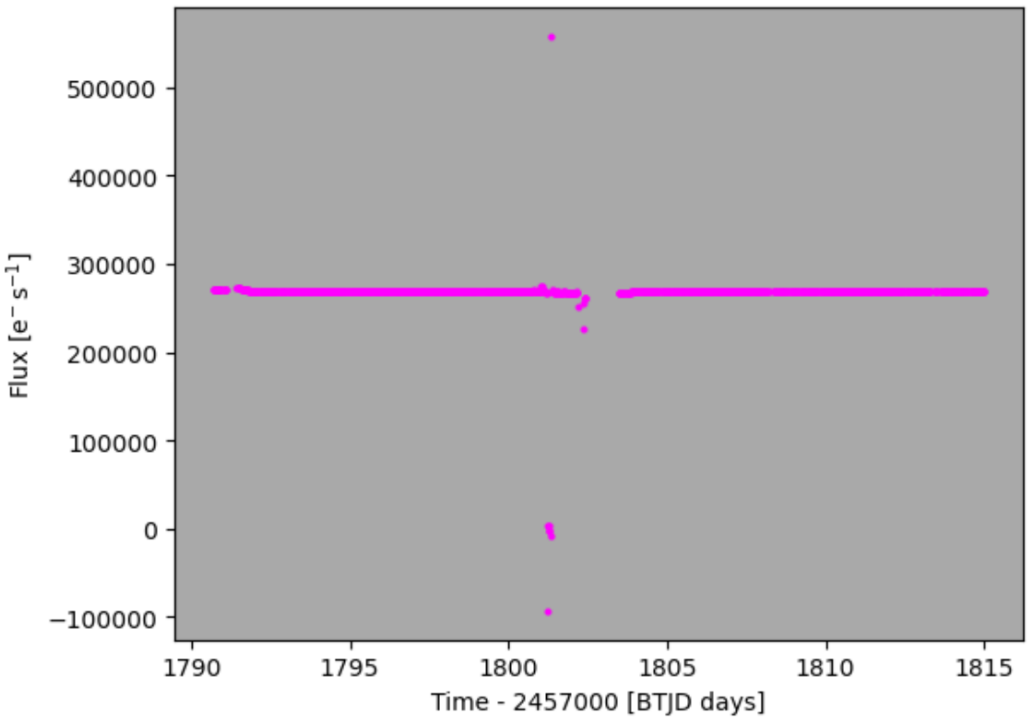

Figure 3.5: *TESS* light curve with eleanor reduction.

3.2.3 Single Transit Working Group

A massive challenge in the earlier stages of this research project was finding hot, bright stars worth observing. When looking at a list of observable F-stars, the selection process was random and often times unfruitful, as is further discussed in chapter 4. To aid in selecting targets, we have considered following up on long period candidates.

One of Wesleyan's astronomy postdoctoral researchers, Dr. Jonathan Jackson, is on *TESS*'s single transit working group. The working group identifies single transits detected by *TESS*. From there, I'm able to use MAST to view these light curves and determine the proper steps for a follow up observation using Wesleyan's telescope.

Chapter 4

Results

4.1 HD 21844

4.1.1 Candidate Transit Events

HD 21844 is an F-Type star with a V magnitude of 6.59 (Høg et al. 2000) and an effective temperature of 6816 K (Casagrande et al. 2011). Additionally, it is a binary star (Gaia Collaboration 2022), meaning that it is comprised of two stars orbiting each other. As shown in Table 4.1, we have observed the star for 36 nights, with most of these nights showing little stellar flux variation. On the night of 2022 January 25, however, Cassidy Soloff observed what looked like a partial planetary transit around HD 21844.

Figure 4.1 shows this observation, with what appears to be an almost complete transit at the end of the night. This transit shape can be more clearly seen when the data points are binned, or averaged over discrete time intervals. Figure 4.2 shows the original data points, observed every 0.8 seconds, and 50 averaged data points, represented by the large symbols. Using the Python package `batman`

Star	Nights Observed	Hours Observed
HD 21844	36 days	67.21 hrs

Table 4.1: Number of nights and hours that HD 21844 has been observed for.

(Kreidberg 2015), a transit curve modeling tool, we can further verify that the light curve has a transit shape, as seen in Figure 4.3. On the night of 2022 November 2, I observed HD 21844. The reduced data is shown in Figure 4.4.

At first glance, there is a notable "jump" a third of the way through the observation, as indicated by the red line. This feature arose as the result of an error in data reduction, which stemmed from how HD 21844 was observed. Over any given observation, exposures are not taken continuously. In this case, they were taken in 100 frame increments. Between these increments, the scheduler took time to re-input the observation instructions, which led to a discontinuity in the position of stars relative to the telescope. This caused the stars' image positions between each increment to "jump." Consequently, during data reduction in AstroImageJ, aperture positions had to be manually reset each 100 frames to account for the stars shifting. With this data set, I made a mistake with my aperture placements between one of the increments, which resulted in a discontinuity in the reduced data. Recognizing this error, I corrected the data processing and ended up with a dip in flux, consistent with the partial transit candidate that Cassidy observed.

The dip can be more clearly seen with binned data points, shown in Figure 4.5. This data set also closely matched the same `batman` curve that Cassidy generated for the January transit shown in Figure 4.6. The similarity between these two candidate transit events can be seen when one is placed atop the other, as shown in Figure 4.7. Combining everything together in Figure 4.8, we see how strong the correlation between these two light curves is.

On the night of 2022 December 8, I observed what looked like a transit around HD 21844. This data can be seen in Figure 4.9. The similar depth to previous observations seemed to indicate another promising transit candidate. However, there were more correlation tests to be conducted before that could be determined.

The first step was to overlay the `batman` curve and see if there was a match. As seen in Figure 4.10, the overlay showed a decent depth correlation, but the duration of the transit candidate event was much shorter than the model curve. At this point, the final test was to see how this curve looked against the first transit candidate event from 25 January 2022.

As is evident from Figure 4.11, there are significant differences between the candidate transit events from January and December. Despite the depths matching decently, the durations are quite different, which immediately shows a lack of correlation. This leaves us with the only complementary light curves being those from January and November. Even though we only have two, there is a good amount that can be done to narrow the search for more transits.

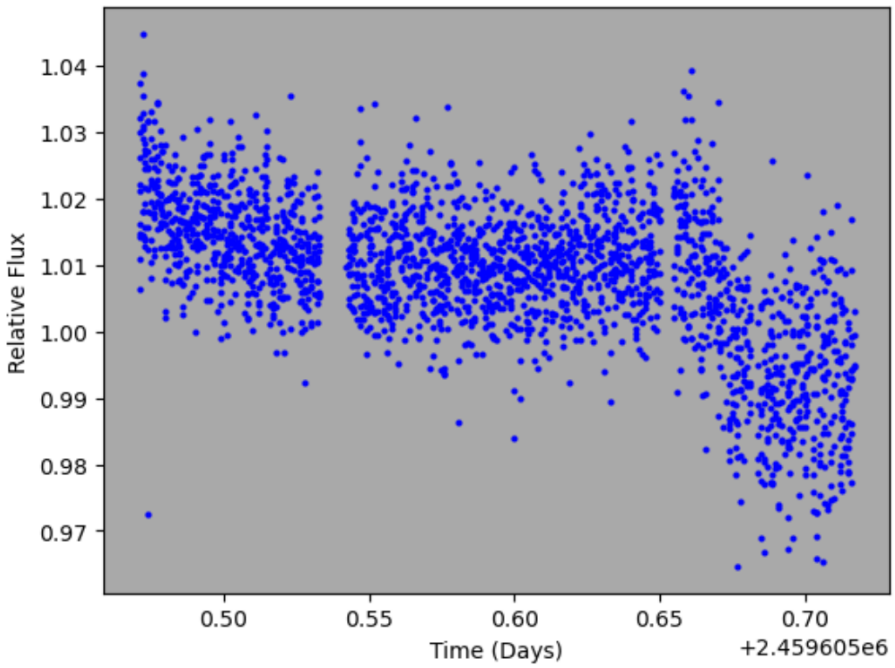

Figure 4.1: Raw data from the possible transit observed on 2022 January 25.

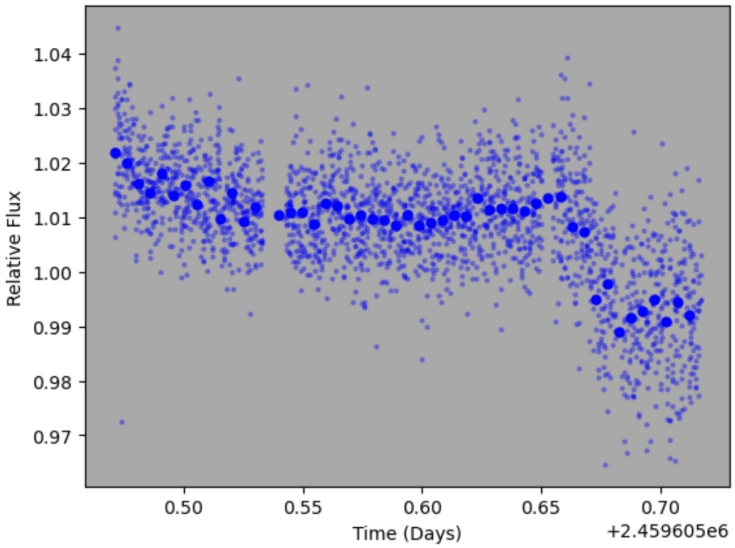

Figure 4.2: Raw data from 2022 January 25 with binned points overlaid.

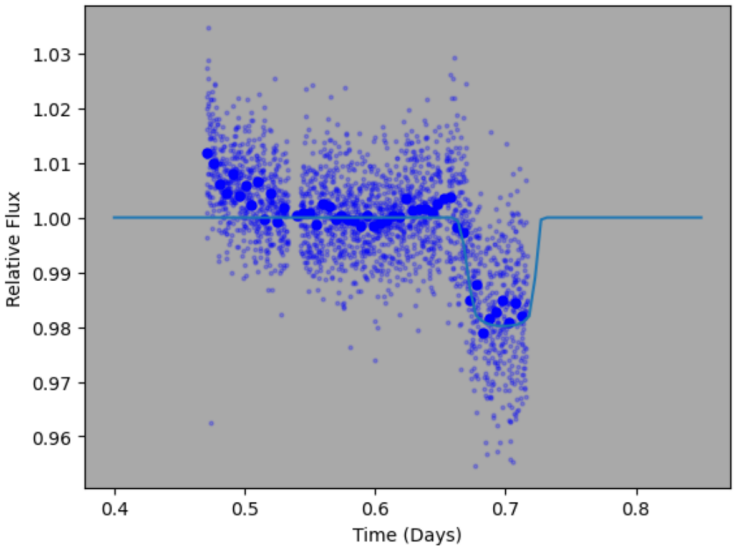

Figure 4.3: Data taken on 2022 January 25 with a curve fit using the python package `batman`.

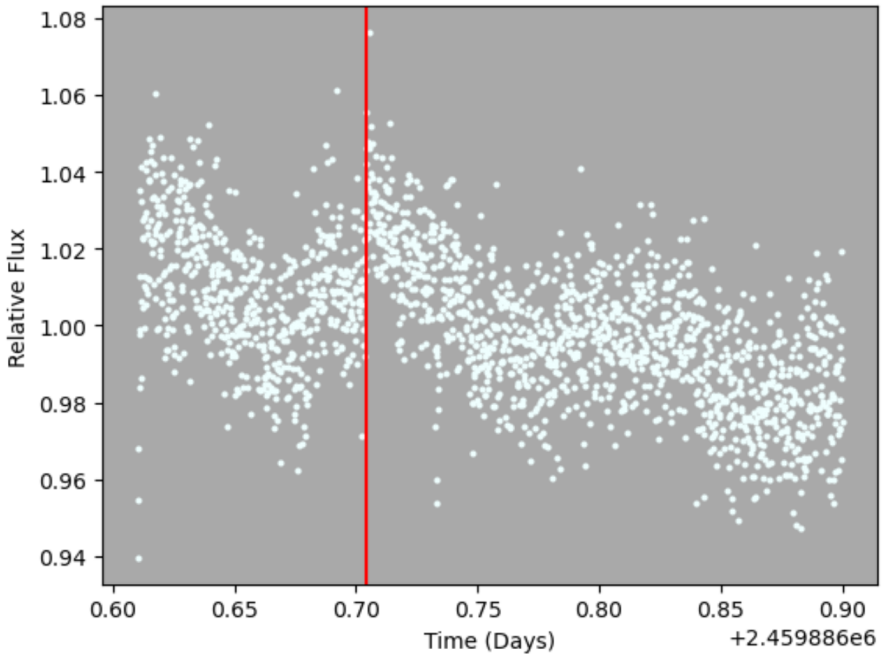

Figure 4.4: Raw data from the possible transit observed on 2022 November 2.

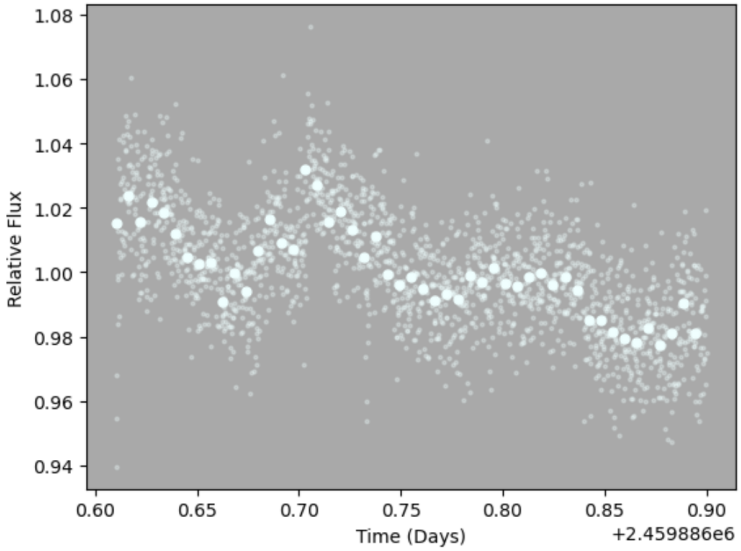

Figure 4.5: Raw data from 2022 November 2 with binned points overlaid.

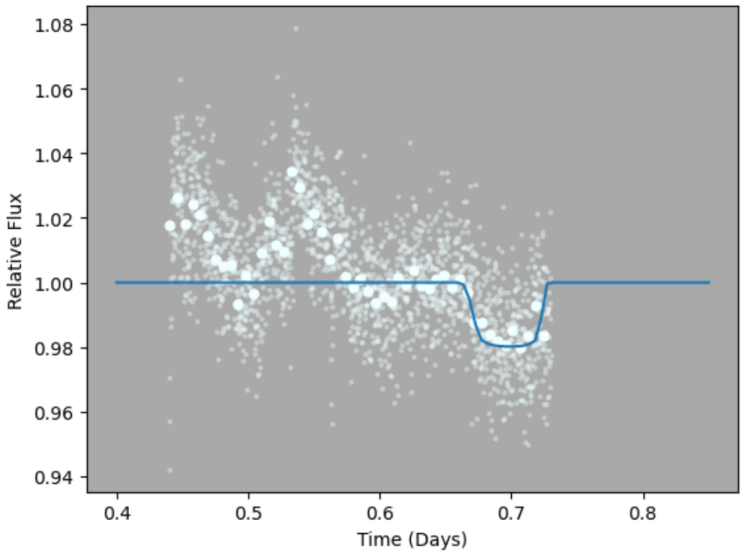

Figure 4.6: Data taken on 2022 November 2 with a curve fit using the python package `batman`.

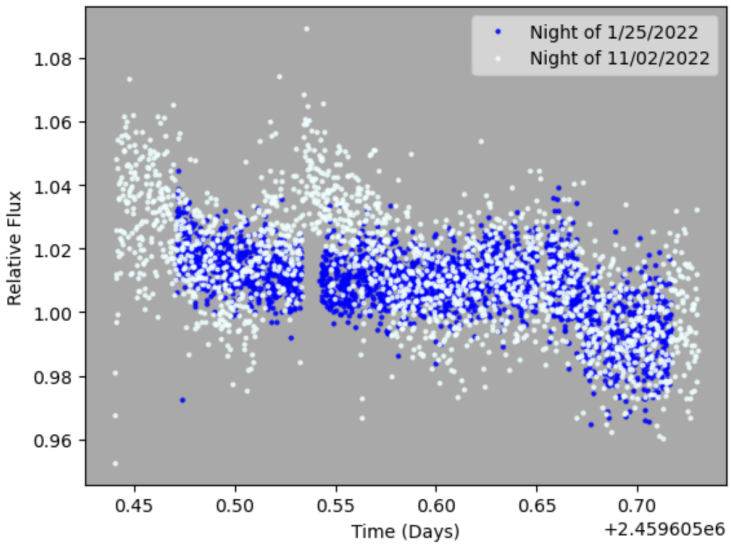

Figure 4.7: Raw data from both transits.

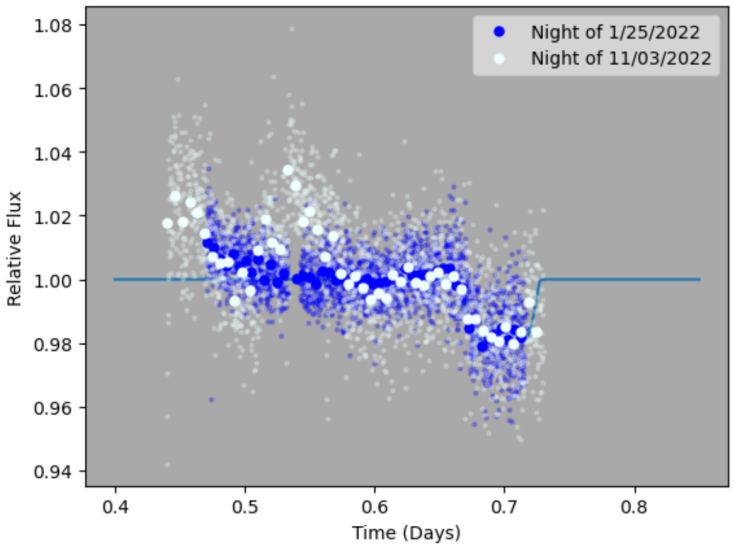

Figure 4.8: Data from both transits with a curve fit.

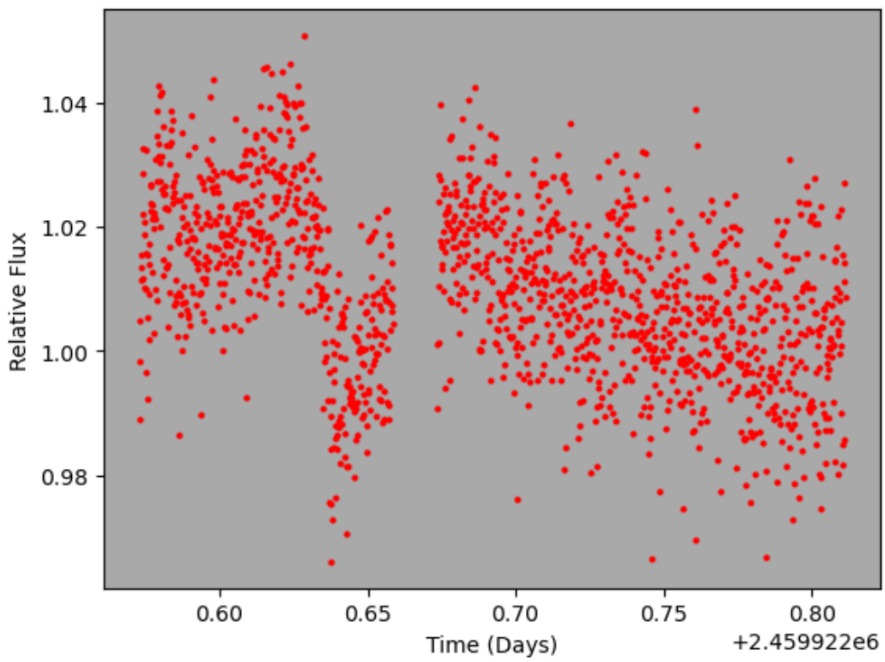

Figure 4.9: Raw data from the false-positive transit observed on the night of 2022 December 8.

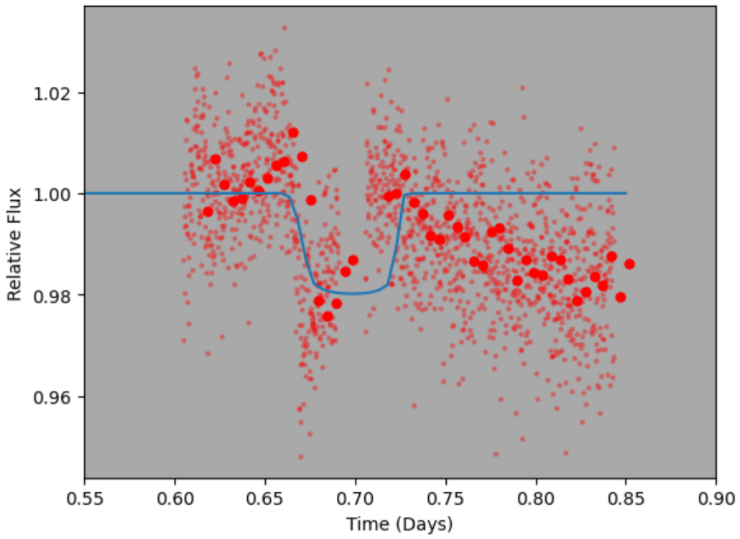

Figure 4.10: Data taken on 2022 December 8 with a curve fit using the python package `batman`.

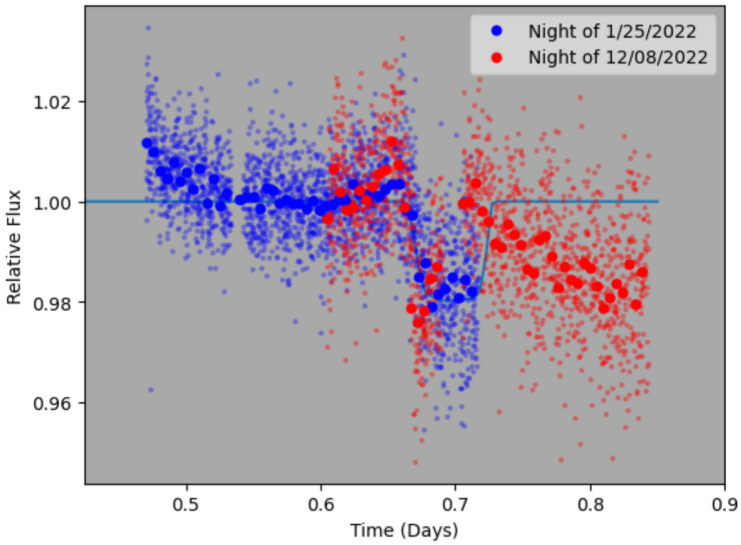

Figure 4.11: Data from both transits with a curve fit.

4.1.2 Stellar Binarity of HD 21844

Firstly, a potentially confounding variable must be addressed. HD 21844 is a binary star (Gaia Collaboration 2022), which introduces the possibility that the orbital behavior of this binary could be responsible for the light curves that have been observed. As opposed to a planet, the dimmer star in the binary could have passed in front of the brighter one to create the flux dips that we observed.

This can be verified by comparing the periodicity of the binary orbit (588.909 ± 9.061 days) with the time between the two transit candidates as well as the false-positive candidate.

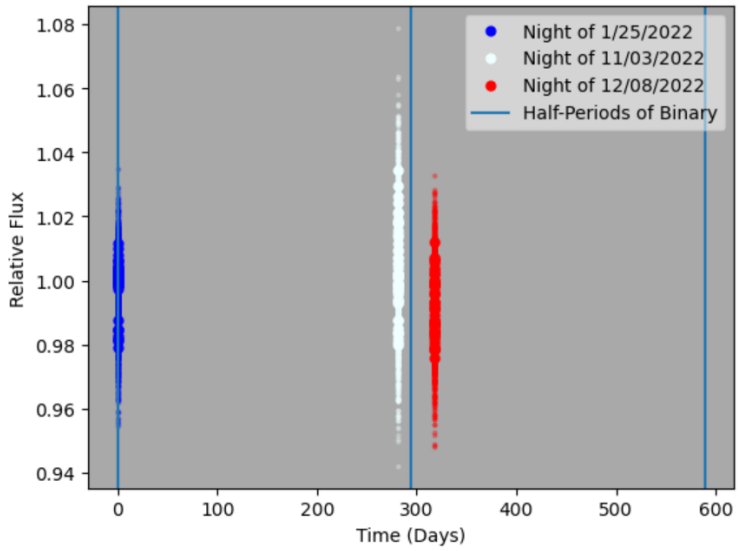

Figure 4.12: Data from the January, November, and December observations with lines representing each half-period of the HD 21844 binary.

As the Figure 4.12 shows, the closest that the transit candidates come to coinciding with the binary's periodicity is at a half period. In that case, the time between that half period and the closest transit candidate is 13.540 days, about 1.5 times the standard error. This points to a lack of influence of HD 21844's binary orbit on the data collected.

4.1.3 Determining the Planetary Period for HD 21844

Along with the data collected at Wesleyan, *TESS* has also observed HD 21844, as can be seen in Figure 4.13.

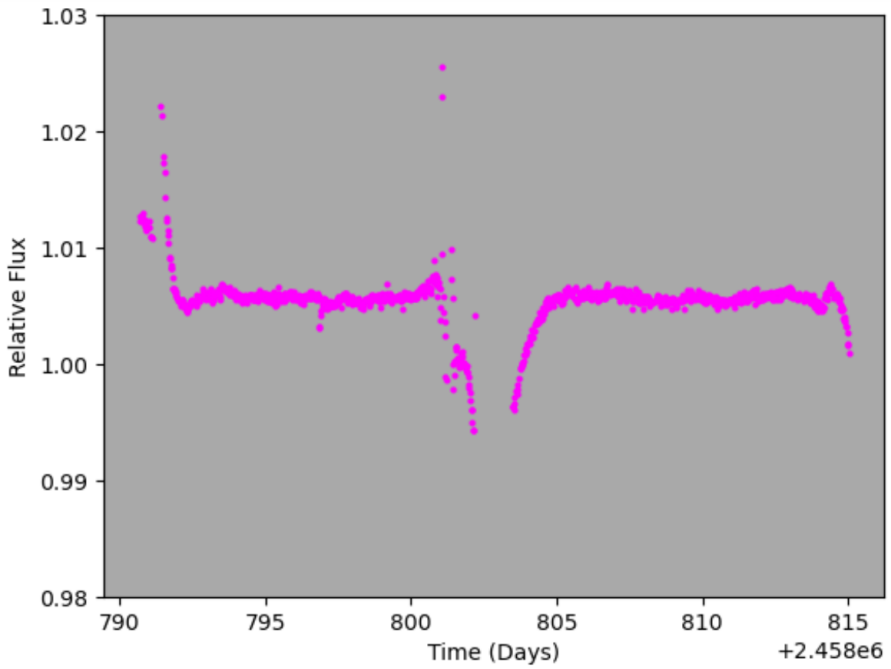

Figure 4.13: Data from *TESS*'s observation of HD 21844.

This data is largely stable, showing no significant variations other than those caused by the instrumentation beginning, stopping, or continuing the observation. While it does not contain any transits, it is still incredibly useful for period predictions.

Given our observation of two transit candidates, a maximum period can be determined for this potential planet (281.17 days), but the frequency at which this candidate exoplanet orbits is unknown. As such, we know that the "true" period must be the maximum period divided by some integer. With this principle in mind, we can check various period frequencies and determine whether they

intersect with observations that yielded no transits. If they do, we can eliminate them as a possibility.

A problem that occurs with this method when using only Wesleyan's data is that the telescope can only observe during the nighttime, meaning that many of the period frequencies fall between observations; thus, it becomes difficult to rule them out. Fortunately, *TESS* is incredibly useful with this, providing long-duration, continuous data, that allows for many more frequencies to be ruled out.

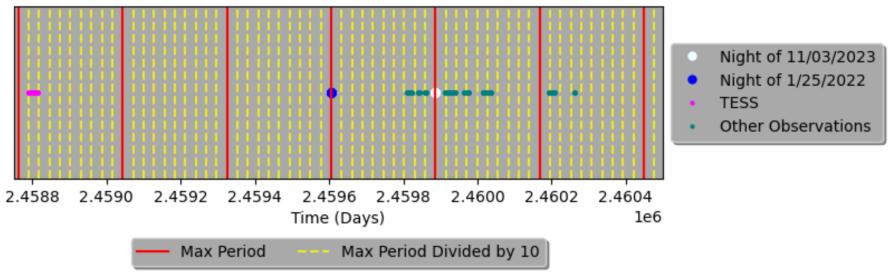

Figure 4.14: HD 21844 data tested against a period frequency of 10 orbits per maximum period.

So far, the most viable frequencies are 1,2,3,4,5, and 10 orbits (shown in Figure 4.14) per maximum period. This is due to the other period frequencies intersecting with HD 21844's observations, either from *TESS* or Wesleyan's 24-inch telescope. The observation dates corresponding to the remaining possible frequencies in UTC (Coordinated Universal Time) can be seen in Table 4.2.

Table 4.2: UT Date and Time of Next Transit

P=281.17d n=1	P=140.59d n=2	P=93.72d n=3	P=70.29d n=4	P=56.23d n=5	P=28.11d n=10
2024 May 18 16:03	2024 May 18 16:03	2024 Feb 14 22:41	2024 Mar 09 09:02	2024 Jan 27 04:49	2024 Jan 27 04:49
2025 Feb 23 20:08	2024 Oct 06 06:05	2024 May 18 16:03	2024 May 18 16:03	2024 Mar 23 10:26	2024 Feb 24 07:37
2025 Dec 02 00:12	2025 Feb 23 20:08	2024 Aug 20 09:24	2024 Jul 27 23:04	2024 May 18 16:03	2024 Mar 23 10:26
2026 Sep 09 04:17	2025 Jul 14 10:10	2024 Nov 22 02:46	2024 Oct 06 06:05	2024 Jul 13 21:40	2024 Apr 20 13:14
2027 Jun 17 08:22	2025 Dec 02 00:12	2025 Feb 23 20:08	2024 Dec 15 13:06	2024 Sep 08 03:17	2024 May 18 16:03
2028 Mar 24 12:27	2026 Apr 21 14:15	2025 May 28 13:29	2025 Feb 23 20:08	2024 Nov 03 08:54	2024 Jun 15 18:51
2028 Dec 30 16:32	2026 Sep 09 04:17	2025 Aug 30 06:51	2025 May 05 03:09	2024 Dec 29 14:31	2024 Jul 13 21:40
2029 Oct 07 20:36	2027 Jan 27 18:20	2025 Dec 02 00:12	2025 Jul 14 10:10	2025 Feb 23 20:08	2024 Aug 11 00:28
2030 Jul 16 00:41	2027 Jun 17 08:22	2026 Mar 05 17:34	2025 Sep 22 17:11	2025 Apr 21 01:45	2024 Sep 08 03:17
2031 Apr 23 04:46	2027 Nov 04 22:24	2026 Jun 07 10:56	2025 Dec 02 00:12	2025 Jun 16 07:21	2024 Oct 06 06:05
2032 Jan 29 08:51	2028 Mar 24 12:27	2026 Sep 09 04:17	2026 Feb 10 07:14	2025 Aug 11 12:58	2024 Nov 03 08:54
2032 Nov 05 12:56	2028 Aug 12 02:29	2026 Dec 11 21:39	2026 Apr 21 14:15	2025 Oct 06 18:35	2024 Dec 01 11:42
2033 Aug 13 17:00	2028 Dec 30 16:32	2027 Mar 15 15:00	2026 Jun 30 21:16	2025 Dec 02 00:12	2024 Dec 29 14:31
2034 May 21 21:05	2029 May 20 06:34	2027 Jun 17 08:22	2026 Sep 09 04:17	2026 Jan 27 05:49	2025 Jan 26 17:19

The next step for HD 21844 is to observe as many of the dates listed in Table 4.1. At Van Vleck Observatory, some of these dates occur during the night. However, in the case that we are able to access a telescope elsewhere or collaborate with others in different time zones, these dates could still be of use. Observing these dates will lead to further period constraining and possibly lead to another transit observation.

Star	V Mag	Spectral Type	Distance	Effective Temperature	Binary Period
HD 154099	6.290	F0V	102.739 pc	7534 K	N/A
HD 197101	6.450	F2Vn	120.783 pc	6902 K	N/A
HD 8634	6.187	F6V	72.183 pc	6520 K	5.429 d
HD 223552	6.472	F3V	40.935 pc	6723 K	N/A

Table 4.3: Stars observed in June and July 2023 at Van Vleck Observatory. (Oja 1991) (Cowley et al. 1969) (Zorec & Royer 2012) (Gaia Collaboration 2020) (Cowley & Fraquelli 1974) (Gaia Collaboration 2022) (Luck 2017) (Høg et al. 2000) (Abt 2009) (Casagrande et al. 2011) (Cannon & Pickering 1993)

4.2 Other F-Stars

Using the same list that Cassidy created for observable F-stars, I hand-picked 4 to observe in June and July of 2023: HD 154099, HD 197101, HD 8634, and HD 223552. Their properties can be seen in Table 4.3.

4.2.1 Setting An Upper Bound for Transit Depth

When analyzing stellar flux, it is important to gauge what levels of variation could feasibly be caused by a planetary transit. This necessitates the formulation of an upper bound for an acceptable transit depth. To start, we can look at equation 4.1 (Heller 2019), which approximates the depth of a given transit, depending on the radius of the star (R_p) and the radius of the planet (R_s).

$$\Delta F = \frac{R_p^2}{R_s^2} \tag{4.1}$$

To maximize this value, we need to use the smallest stellar radius while using the largest planetary radius. For the radius of the star, we can use the smallest typical value of an F-star on the main sequence, 1.167 solar radii (Pecaut & Mamajek 2013). For the planet's radius, we can use the radius of HAT-P-67 b,

one of the largest gas giants discovered; it has a radius of 2.085 Jupiter radii (Zhou et al. 2017). Using these values, along with the radii of the sun (695.66 Mm) (Haberreiter et al. 2008) and Jupiter (69.911 Mm) (Vazan et al. 2018), we can calculate a reasonable upper bound for transit depth, as seen in equation 4.2.

$$\Delta F = \frac{(2.085 \cdot 69.911)^2}{(1.167 \cdot 695.660)^2} = 0.032 \tag{4.2}$$

Equation 4.2 gives us an upper bound of around 3%, which allows us to determine the feasibility that the light curves we observe indicate transits.

4.2.2 Light Curve Analysis

The light curve in Figure 4.15 lacks any evidence of a transit, given just how much its measured flux changes, coupled with the lack of an observable transit-like curve. Similarly, Figure 4.16's light curve varies wildly but in a way indicative of noise, rather than a transiting object. The time duration is also too short (around 20 minutes) to make a proper assessment. Barring a few outliers, Figure 4.17's curve is fairly steady, hovering around a relative flux value of 1. There is very likely no transit.

There is a dip in the light curve towards the end of the data Figure 4.18. This dip is an over 13.5 percent drop in flux, far too much for a transiting planet. However, this flux drop could be the result of a binary eclipse, as the period of HD 8634's binary is a short 5.429 days (Gaia Collaboration 2022).

The light curve in Figure 4.19 also has a flux dip towards the end, but again, even a 6% dip is likely too much for an exoplanet transit. Figure 4.20 shows yet another light curve that initially seems promising with a flux dip, yet the dip is far too much for an exoplanet. For the data in Figure 4.21, there simply is not

enough data her to discern any kind of transit behavior. The change in the flux at the end is far too gradual and far too high to indicate a transit.

The last few curves in Figures 4.22, 4.23, 4.24, and 4.25 all drive home a similar point: that HD 223552 exhibits variability that makes searching for a transit using a ground-based telescope difficult. In order to efficiently search for and confirm planetary discoveries, a new method is necessary.

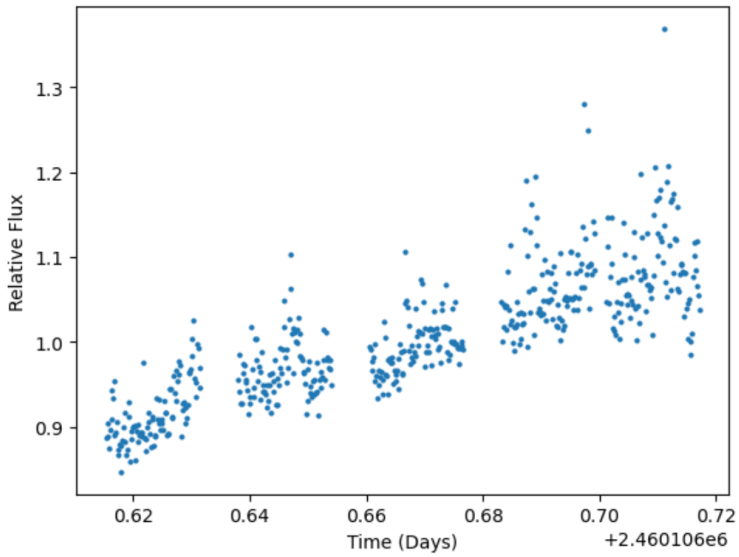

Figure 4.15: HD 154099 data, taken on the night of 2023 June 10.

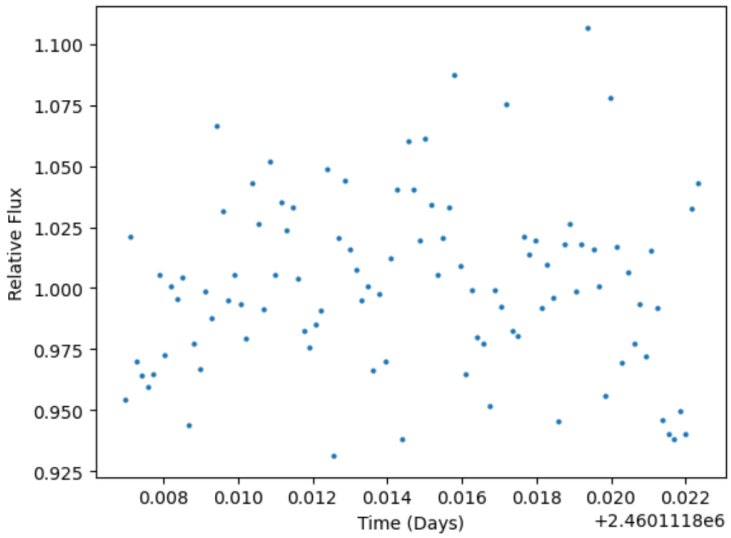

Figure 4.16: HD 154099 data, taken on the night of 2023 June 15.

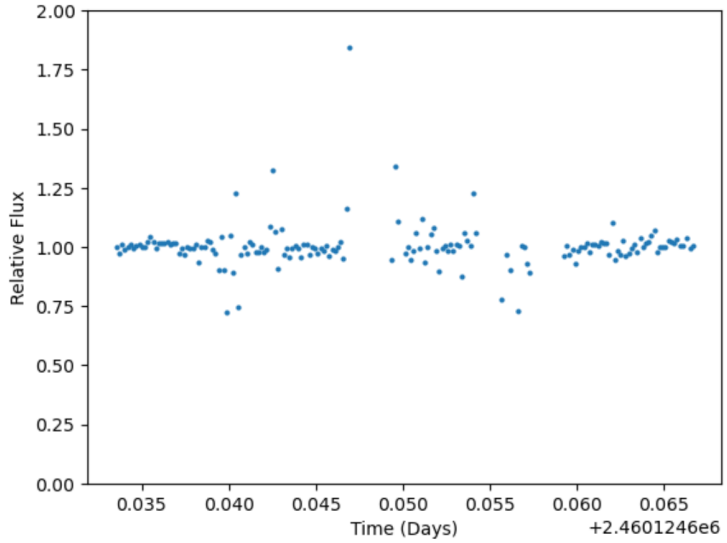

Figure 4.17: HD 197101 data, taken on the night of 2023 June 28.

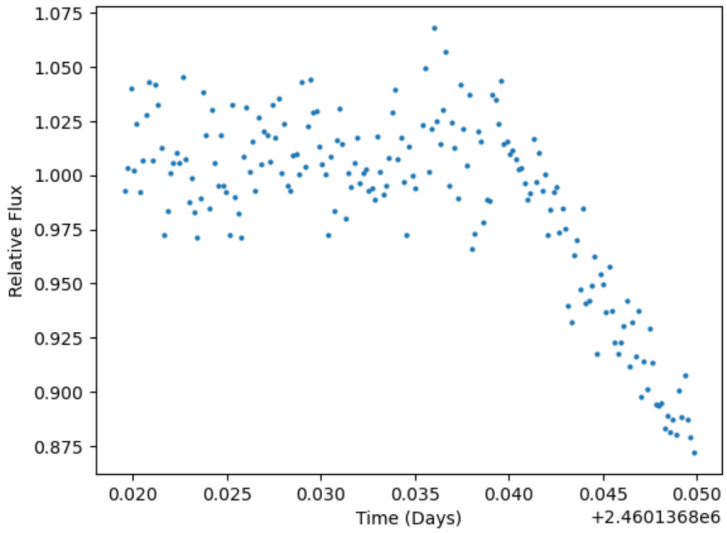

Figure 4.18: HD 8634 data, taken on the night of 2023 July 10.

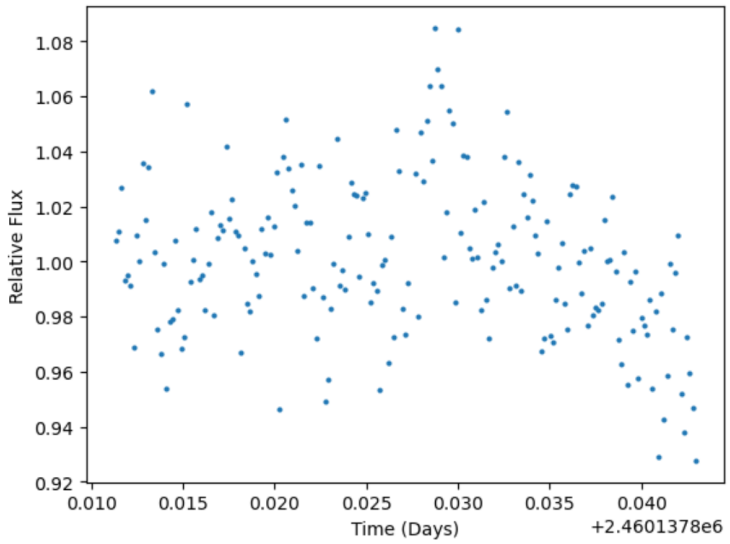

Figure 4.19: HD 8634 data, taken on the night of 2023 July 11.

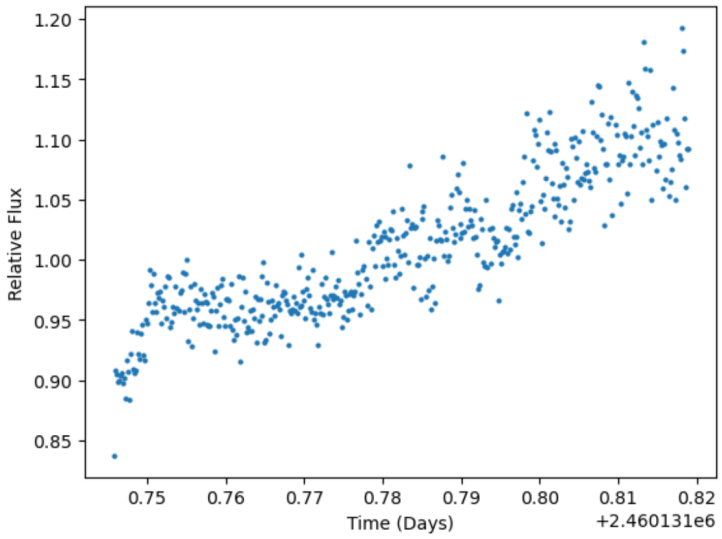

Figure 4.20: HD 223552 data, taken on the night of 2023 July 5.

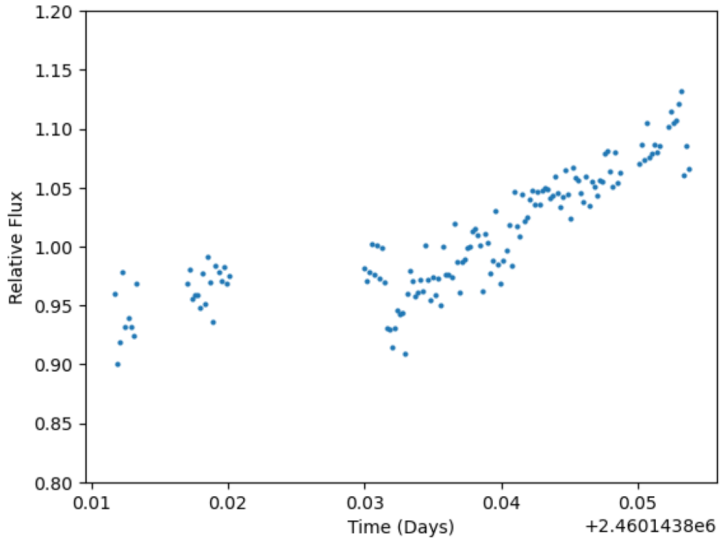

Figure 4.21: HD 223552 data, taken on the night of 2023 July 17.

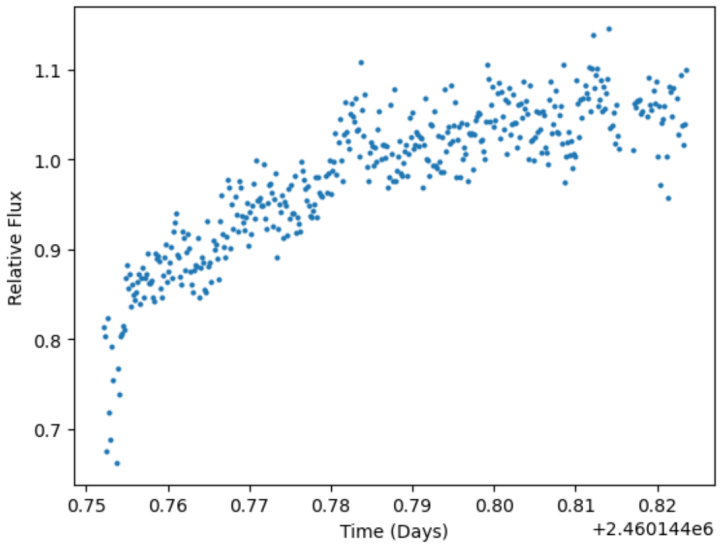

Figure 4.22: HD 223552 data, taken on the night of 2023 July 18.

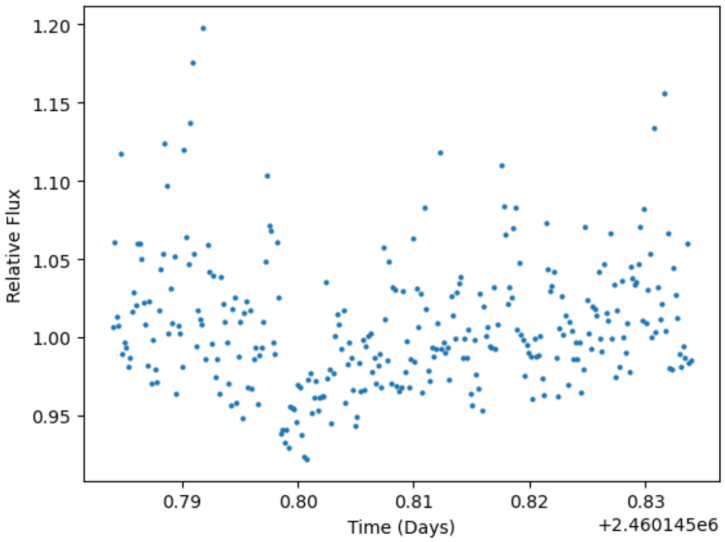

Figure 4.23: HD 223552 data, taken on the night of 2023 July 19.

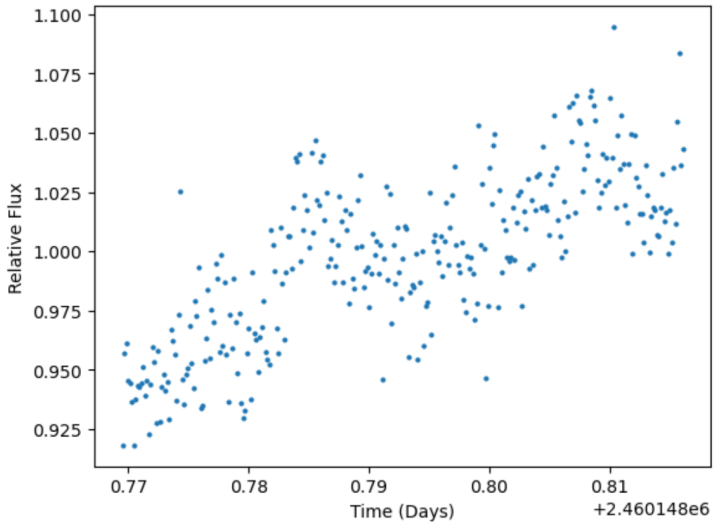

Figure 4.24: HD 223552 data, taken on the night of 2023 July 22.

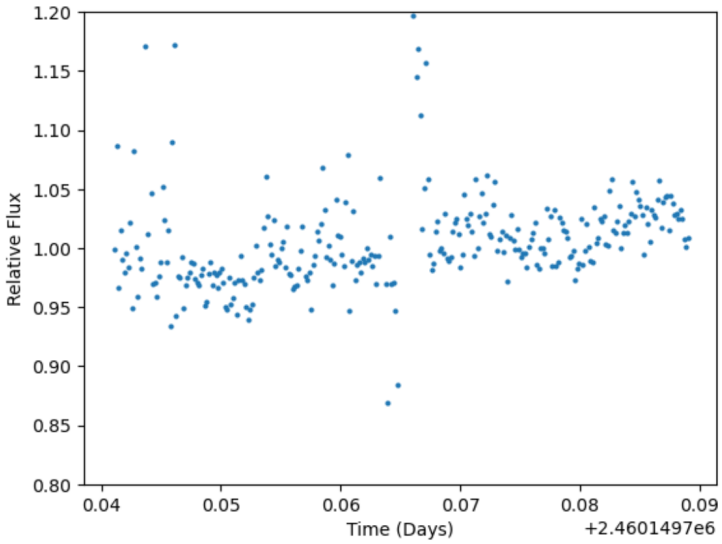

Figure 4.25: HD 223552 data, taken on the night of 2023 July 23.

Star	Nights Observed	Hours Observed
TIC 66638715	77 days	190.59 hrs

Table 4.4: Number of nights and hours that TIC 66638715 has been observed for.

4.3 TIC 66638715

As stated in chapter 3, one of Wesleyan's astronomy postdoctoral researchers, Dr. Jonathan Jackson, is on the *TESS* Single-Transit Working Group. This connection has allowed us to have access to hot, bright stars with observed transits that we can follow up on. For this research project, Dr. Jackson, provided 4 targets that show a single transit event in a single TESS sector length of 27 days. Of the 4, TIC 66638715 was chosen to be observed using Wesleyan's telescope. This was due to the others' transits being less discernible given their data quality. TIC 66638715, however, had a transit that could immediately be spotted, which made it the most desirable candidate for observation. This data can be seen in Figure 4.26.

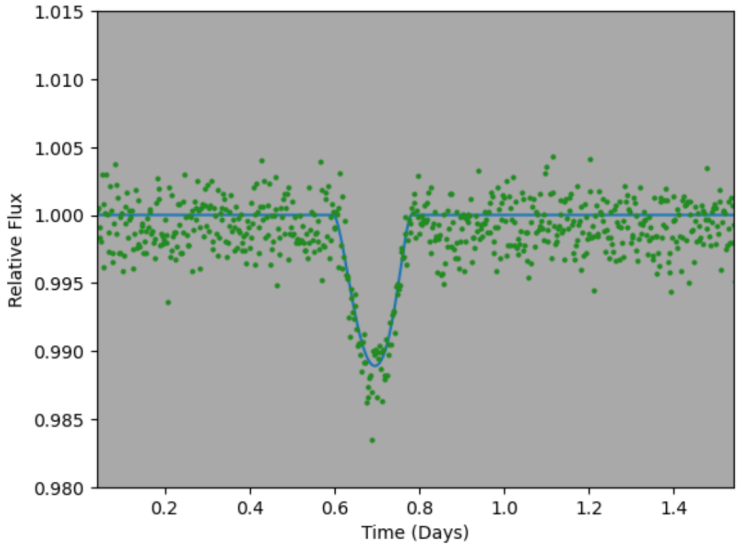

Figure 4.26: TIC 66638715 data taken by *TESS*.

Since then, we have observed TIC 66638715 for 77 nights, searching for another transit, as shown in Table 4.4. While we have not yet spotted one, we know we have the data quality to detect it, as shown in Figure 4.27. Plotting the same `batman` curve as in Figure 4.26, we see that the transit is able to cut through the noise. In the event that another transit is found, we will be able to do the same operations on the data as HD 21844 to determine a periodicity.

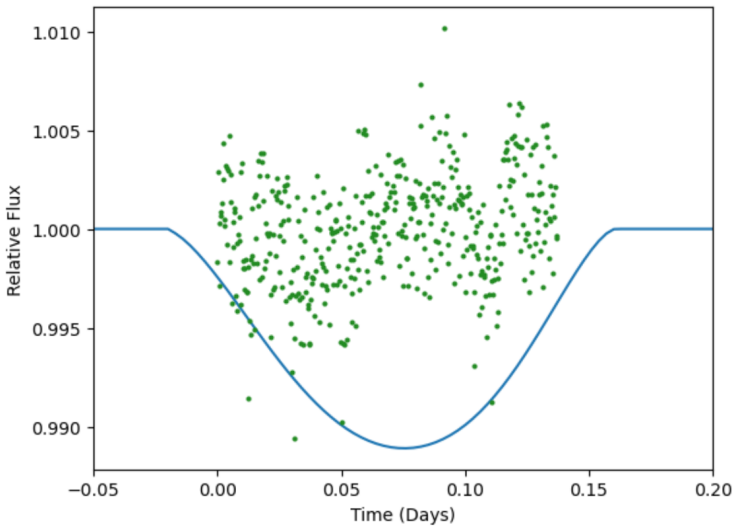

Figure 4.27: TIC 66638715 data taken using Wesleyan's telescope.

Despite not having multiple transits, *TESS*'s continuous 27 day observation still allows us to formulate a lower bound for the transit period. The longest stretch between a *TESS* data point and the transit is 19.29 days, which means that it is the lower limit for what the transit period could be. This information will be useful when another transit of TIC 66638715 is observed, allowing for the elimination of high transit frequencies, as has been done for HD 21844.

Chapter 5

Conclusions and Future Work

Thus far, we have been able to use Wesleyan's 24-inch telescope to observe two candidate transits around a hot, bright F-star (HD 21844) that could indicate the presence of a Jupiter-sized planet in its orbit. Both appear to be partial transits that have a depth of about 2%. These candidate transits, having occurred on 2022 January 25 and 2022 November 2, are spaced 281.17 days apart, meaning that this is their maximum possible period.

Consequently, we have tested different period frequencies against observational data from Wesleyan as well as *TESS* to determine what periods are possible. As of now, there are six: 281.17 days, 140.59 days, 93.72 days, 70.29 days, 56.23 days, and 28.11 days. In order to determine the viability of these periods, HD 21844 needs to be observed on days that intersect with them. Some of these dates line up with favorable observing conditions like time of day and season, whereas others do not. In those cases, there exists the possibility of collaboration or perhaps accessing other telescopes in different time zones.

Alongside HD 21844, we have also started collecting photometric data from another hot star, TIC 66638715, whose *TESS* lightcurve also points to the presence of a similar type of planet. We have observed the star for 77 nights, with a total of 190.59 hours observed. The data we have reduced shows no transit candidates, but we are confident that Wesleyan's telescope will be sensitive enough to detect

a transit when one occurs. Because we only have a single transit, our analysis of the transit period is limited. However, given the length and continuity of the *TESS* data, we have been able to determine that the period must be greater than 19.29 days.

In the immediate future, the priority for those continuing this research is to observe full transits of both HD 21844 and TIC 66638715. For HD 21844, a full transit observation would both add legitimacy to the existence of a hot Jupiter in its orbit, as well as provide data to further constrain the transit period. In the case of TIC 66638715, the observation of a second transit would allow for the same period analysis that HD 21844 has undergone, and future observations would have set dates as opposed to occurring every observable night.

As this research project moves forward, it is important to develop a more formalized pipeline for starting and continuing observations. Thus far, we have barely realized the potential of using *TESS* single transits to inform the discovery of hot Jupiters around hot, bright stars. As more of these targets are observed, there will need to be a more robust system in place to handle the observation, data reduction, and analysis of multiple targets. If this is achieved, researchers at Wesleyan could discover myriad hot Jupiters, setting the foundation to better understand the machinations of these great gas giants that inhabit our universe.

"Life is not a problem to be solved, but a reality to be experienced."

–Søren Kierkegaard

Bibliography

Abt, H. A. 2009, ApJS, 180, 117

Baruteau, C., et al. 2014, in Protostars and Planets VI, ed. H. Beuther, R. S. Klessen, C. P. Dullemond, & T. Henning, 667–689

Borucki, W. J., Dunham, E. W., Koch, D. G., Cochran, W. D., Rose, J. D., Cullers, D. K., Granados, A., & Jenkins, J. M. 1996, Ap&SS, 241, 111

Cannon, A. J., & Pickering, E. C. 1993, VizieR Online Data Catalog: Henry Draper Catalogue and Extension (Cannon+ 1918-1924; ADC 1989), VizieR On-line Data Catalog: III/135A. Originally published in: Harv. Ann. 91-100 (1918-1924)

Casagrande, L., Schönrich, R., Asplund, M., Cassisi, S., Ramírez, I., Meléndez, J., Bensby, T., & Feltzing, S. 2011, A&A, 530, A138

Charbonneau, D., Brown, T. M., Latham, D. W., & Mayor, M. 2000, ApJ, 529, L45

Cowley, A., Cowley, C., Jaschek, M., & Jaschek, C. 1969, AJ, 74, 375

Cowley, A., & Fraquelli, D. 1974, PASP, 86, 70

Feinstein, A. D., et al. 2019, PASP, 131, 094502

Fortney, J. J., Dawson, R. I., & Komacek, T. D. 2021, Journal of Geophysical Research: Planets, 126

Gaia Collaboration. 2020, VizieR Online Data Catalog: Gaia EDR3 (Gaia Collaboration, 2020), VizieR On-line Data Catalog: I/350. Originally published in: 2021A&A...649A...1G; doi:10.5270/esa-1ug

—. 2022, VizieR Online Data Catalog: Gaia DR3 Part 3. Non-single stars (Gaia Collaboration, 2022), VizieR On-line Data Catalog: I/357. Originally published in: Astron. Astrophys., in prep. (2022)

Haberreiter, M., Schmutz, W., & Kosovichev, A. G. 2008, The Astrophysical Journal, 675, L53–L56

Heller, R. 2019, A&A, 623, A137

Høg, E., et al. 2000, A&A, 355, L27

Jackson, J. M., Dawson, R. I., Shannon, A., & Petrovich, C. 2021, AJ, 161, 200

Johansen, A., & Lambrechts, M. 2017, Annual Review of Earth and Planetary Sciences, 45, 359

Kreidberg, L. 2015, PASP, 127, 1161

Luck, R. E. 2017, AJ, 153, 21

Maldonado, J., Villaver, E., & Eiroa, C. 2018, AA, 612, A93

Mayor, M., & Queloz, D. 1995, Nature, 378, 355

Oja, T. 1991, A&AS, 89, 415

Pecaut, M. J., & Mamajek, E. E. 2013, ApJS, 208, 9

Ricker, G. R., et al. 2014, Journal of Astronomical Telescopes, Instruments, and Systems, 1, 014003

Rodriguez, J. E., et al. 2016, The Astronomical Journal, 151, 138

Soloff, C., & Redfield, S. 2022, in American Astronomical Society Meeting Abstracts, Vol. 54, American Astronomical Society Meeting #240, 403.13

Swade, D., Fleming, S., Mullally, S., Latham, D., Jenkins, J. M., Morgan, E., & Vanderspek, R. 2019, in Astronomical Society of the Pacific Conference Series, Vol. 523, Astronomical Data Analysis Software and Systems XXVII, ed. P. J. Teuben, M. W. Pound, B. A. Thomas, & E. M. Warner, 453

Vazan, A., Helled, R., & Guillot, T. 2018, A&A, 610, L14

Wells, D. C., Greisen, E. W., & Harten, R. H. 1981, A&AS, 44, 363

Wolszczan, A., & Frail, D. A. 1992, Nature, 355, 145

Yao, X., et al. 2021, The Astronomical Journal, 161, 124

Zhou, G., et al. 2017, AJ, 153, 211

Zorec, J., & Royer, F. 2012, A&A, 537, A120